Muon spin relaxation in YMn_2D_x deuterides

1996 J. Phys.: Condens. Matter 8 4603

(http://iopscience.iop.org/0953-8984/8/25/016)

J. Phys.: Condens. Matter **8** (1996) 4603–4615. Printed in the UK

Muon spin relaxation in YMn_2D_x deuterides

M Latroche†, H Figiel‡, G Wiesinger§, Cz Kapusta‡, P Mietniowski‡, V Paul-Boncour†, A Percheron-Guegan† and R Cywinski‖

† LCMSTR, UPR 209, CNRS 1 place Aristide Briand, 92195 Meudon Cédex, France
‡ Department of Solid State Physics, University of Mining and Metallurgy, Al. Mickiewicza 30, 30-059 Krakow, Poland
§ Institute of Experimental Physics, Technical University, Wiedner Haupstrasse 8-10, A-1040, Wien, Austria
‖ Department of Physics and Astronomy, University of St Andrews, St Andrews, Fife KY16 9SS, UK

Received 24 October 1995, in final form 29 February 1996

Abstract. Zero- and longitudinal-field muon spin relaxation techniques have been used to study spin fluctuations in YMn_2D and YMn_2D_2 compounds in the temperature range 10–300 K. The temperature dependence of the asymmetry parameter indicates a first-order transition to ferrimagnetism at $T_c = 220$ K and 260 K for YMn_2D_1 and YMn_2D_2, respectively. In contrast the depolarization rate $\lambda(T)$ exhibits a critical divergence, characteristic of a continuous transition, as T_c is approached from above. These features are consistent with those observed for the parent compound YMn_2 and indicate that the character of the spin fluctuations in the paramagnetic state changes little with deuterium loading, despite marked modifications to the low-temperature, magnetically ordered state. $\lambda(T)$ provides evidence of significant spin fluctuations below T_c, while slight deviations from predicted behaviour indicate further structural or magnetic transitions in the ordered state.

1. Introduction

The interaction of hydrogen with materials is a subject of considerable scientific and technological interest. Rare-earth (R)–3d transition-metal (T) intermetallic compounds are often used as model systems in which this interaction can be investigated [1]; they readily absorb hydrogen, leading to substantial modifications of their physical properties. In the case of the RT_2 Laves phase compounds with T = Mn, these modifications have proved both dramatic and intriguing [2]. In the parent RMn_2 compounds the Mn moment is hypersensitive to the cell volume; hydrogen incorporation at interstitial sites can therefore induce changes in the degree of localization and magnitude of the Mn moment, the orbital contribution to the moment, the hyperfine parameters and also the ground-state magnetic structure.

For example, the C15 Laves compound YMn_2 is an itinerant-electron spin-fluctuating paramagnet at high temperatures [3]. On cooling below 100 K the compound exhibits a first-order transition to an antiferromagnetic helix with approximately $3\mu_B$ localized at each Mn site. The onset of magnetic order is accompanied by a structural transition, characterized by a discontinuous 5% increase in the cell volume. Recently, heavy-fermion features were also reported for this intermetallic compound [4]. Hydrogenation of YMn_2 produces single-phase hydrides YMn_2H_x for $1 < x < 3.5$ with the hydrogen atoms

0953-8984/96/254603+13$19.50

occupying preferentially a tetrahedral site surrounded by two yttrium and two manganese sites. These hydrides maintain the cubic C15 structure down to liquid-helium temperature, while exhibiting a continuous increase in the lattice parameter with increasing hydrogen content [5, 6]. However, hydrogen absorption leads to a ferrimagnetic, rather than an antiferromagnetic, ground state in which both the Curie temperature and the Mn moment increase with increasing hydrogen content up to 3 H mol^{-1} [7].

Muon spin rotation and relaxation (μSR) have been instrumental in establishing the role of spin fluctuations in defining the magnetic and structural properties of YMn_2 [8, 9]. We have now used zero- and longitudinal-field μSR techniques to elucidate the spin dynamics and magnetic order in the related deuterides YMn_2D_1 and YMn_2D_2.

2. Experimental details

The samples studied in these μSR measurements were prepared as deuterides rather than hydrides in order to facilitate complementary neutron diffraction experiments on the same material.

Initially, the YMn_2 parent compound was fabricated from high-purity materials in a standard induction furnace. This compound was then deuterated in a constant-volume apparatus, the amount of absorbed deuterium being determined by the change in deuterium gas pressure. X-ray diffraction showed the resulting YMn_2D and YMn_2D_2 powders to be single phase with the C15 structure. μSR samples were prepared as discs of 25 mm diameter and 2 mm thick by packing the YMn_2D_x powder, under a controlled atmosphere, into aluminium sample holders and finally sealing in kapton.

The $^{+}\mu$SR experiments were performed on the MuSR instrument [10, 11] at the ISIS facility at the Rutherford Appleton Laboratory. The pulsed muon beam at ISIS has a repetition rate of 50 Hz and a pulse width of 70 ns. Measurements were made in longitudinal geometry in which the longitudinal relaxation function $G_z(t)$ is obtained by monitoring the time dependence of the muon decay asymmetry using detector arrays in the forward (F) and backward (B) directions. Explicitly $G_z(t)$ is determined from the F and B positron count rates $N_{F/B}(t)$ using the expression

$$\frac{N_F(t) - \alpha N_B(t)}{N_F(t) + \alpha N_B(t)} = a_0 G_z(t). \tag{1}$$

a_0 is the initial asymmetry, typically taking the value of 0.25 on MuSR. The calibration constant α corrects for the relative efficiencies of the F and B detector arrays. Both α and the zero-time offset t_0 are determined from the muon precession signal observed when applying a 2 mT transverse field to the samples. Measurements of $G_z(t)$ were made with the samples in zero field and in longitudinal applied fields of up to 200 mT.

The YMn_2D_x samples were mounted on the cold finger of a closed-cycle refrigerator (CCR), thus permitting temperature scans over the range 15 K $< T <$ 340 K. The sample holder was masked from the muon beam by a silver plate with a 25 mm aperture. The muon mobility in silver results in extreme motional narrowing of the muon relaxation, and hence the background signal resulting from muons stopping in the silver plate is independent of time t. In the present experiment the background b, resulting from muons stopping outside the area of the sample contributed approximately 0.03 to the total observed asymmetry of 0.25.

3. Results and discussion

All the relaxation spectra observed from both samples at all temperatures were described by the functional form

$$a_0 G_z(t) = a_1 \exp(-\lambda t) + b. \tag{2}$$

A very fast depolarization in the μSR signal is clearly seen on a short time scale. This component, which extends over a first few time channels (i.e. approximately the first 50 ns) of the spectra, is an artefact of the t_0 calibration and spectrum normalization procedures. It is therefore excluded from all subsequent data analysis.

Such exponential relaxation implies the presence of rapidly fluctuating magnetic fields at the muon site. The muon depolarization rate λ in this case is related to the relaxation time τ_c of the fields via the relation $\lambda = 2\gamma_m^2 \langle B^2 \rangle \tau_c$ [12], where γ_m is the gyromagnetic ratio of the muon. In fitting the exponential relaxation function to the spectra, the initial asymmetry a_1 and the depolarization rate λ were free parameters. Typical data, together with the associated fits, are shown in figure 1 for the YMn_2D_1 sample at 220 K and 300 K. The temperature dependences of the asymmetry parameter are shown in figures 2(a) and 3(a) for the YMn_2D_1 and YMn_2D_2 samples, respectively, while the temperature dependences of λ are shown in figures 4(a) and 5(a).

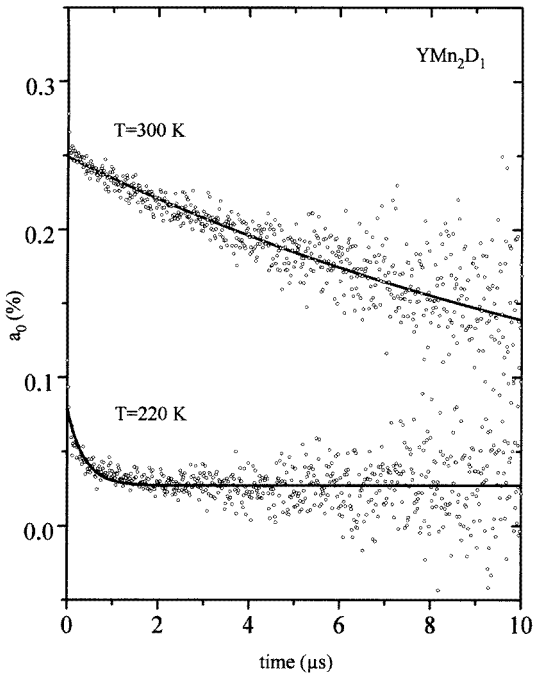

Figure 1. Typical μSR spectra at 220 K (lower curve) and 300 K (upper curve), i.e. at T_c and above T_c for YMn_2D_1. The solid curves represent least-squares fits of equation (2) to the data.

Considering first the behaviour of the initial asymmetry, it can be seen that for both samples a rapid decrease in a_1 is apparent close to the transition temperatures $T_c = 220$ K for YMn_2D_1 and $T_c = 260$ K for YMn_2D_2, observed in magnetization measurements [13] on the respective compounds (figures 2 and 3). This decrease in a_1 can be understood

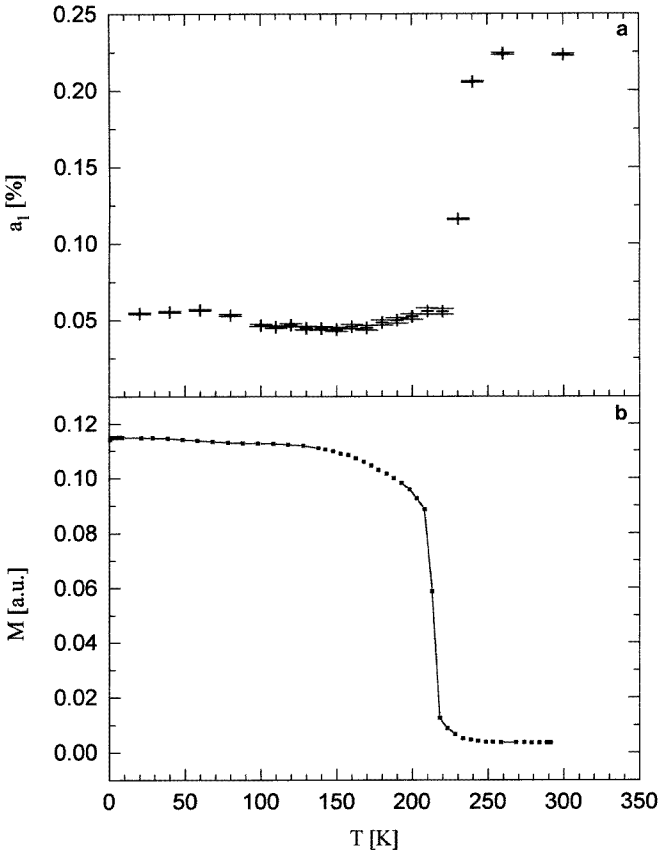

Figure 2. The temperature dependences of (*a*) the asymmetry parameter a_1 and (*b*) the magnetization $M(T)$ (after [13]) for YMn_2D_1 (a.u., arbitrary units).

in terms of a transition to a magnetically ordered state in which the internal field at the muon site is relatively large; for a polycrystalline, magnetically ordered system, the muon relaxation function is given by

$$G(t) = \tfrac{1}{3}G_{-}(t) + \tfrac{2}{3}G_{\perp}(t)\cos(\omega_{\mu}t). \tag{3}$$

The oscillatory term represents muon precession in the presence of internal fields which are orthogonal to the initial muon polarization, while $G_{\perp}(t)$ describes the dephasing of this coherent precession arising from dynamic and static fluctuations of the internal fields. As the time structure of the incident muon pulse at ISIS precludes observation of any oscillatory component in fields much greater than 0.06 T, the exponential relaxation spectra observed below the magnetic transition are therefore associated solely with $G_{-}(t)$. This term results from a purely dynamic depolarization of those muon spins which are initially oriented parallel to the local internal field. At the magnetic transition the initial asymmetry of the observed spectra should thus fall to a third of that of the asymmetry in the paramagnetic state. The value of a_1 observed for both the YMn_2D_1 and the YMn_2D_2 samples at low temperatures is approximately 0.05. This is a little lower than expected from the value in the paramagnetic state ($a_1 = 0.22$) and may reflect some preferred orientation within the powder samples.

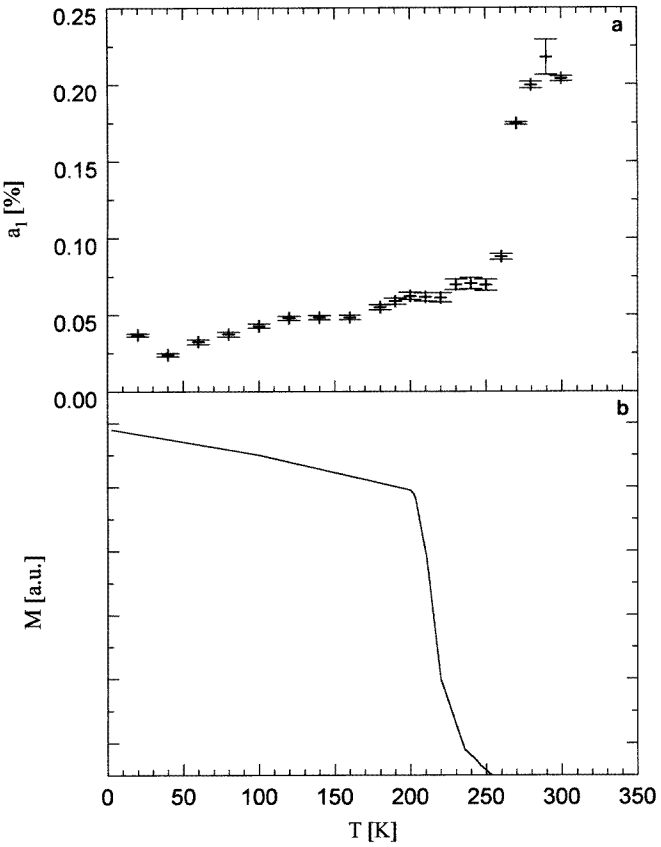

Figure 3. The temperature dependences of (*a*) the asymmetry parameter a_1 and (*b*) the magnetization $M(T)$ (after [13]) for YMn_2D_2.

The temperature dependence of the exponential damping rate λ is presented in figures 4(*a*) and 5(*a*) for the YMn_2D_1 and YMn_2D_2 samples, respectively. For both samples a rapid divergence in λ is observed as the temperature decreases to the critical point T_c. The decrease in λ as the temperature falls below T_c is far less rapid, extending over 100 K. This indicates the presence of significant dynamic depolarization processes, possibly spin waves or residual spin fluctuations, well into the ordered state. It should be noted that the values of λ measured close to T_c (5 μs^{-1} and 20 μs^{-1} for the YMn_2D_1 and YMn_2D_2 samples, respectively) are at the very limits of the resolution of the MuSR spectrometer and must therefore be treated with some caution. Nevertheless, the transition temperatures obtained from the divergence of λ is in full accord with those obtained from the temperature dependence of a_1. The divergence of λ also corresponds closely to the temperatures at which anomalies are observed in the thermal expansion of the respective compounds, as can be seen in figures 4(*b*) and 5(*b*) where the temperature dependences of the lattice parameters of YMn_2D_1 and YMn_2D_2 are shown.

Longitudinal field μSR spectra were also recorded in fields of up to 200 mT for both the YMn_2D_1 and the YMn_2D_2 samples in the paramagnetic phase, above T_c. It was found that the muon depolarization remained exponential in form, although the damping rate λ

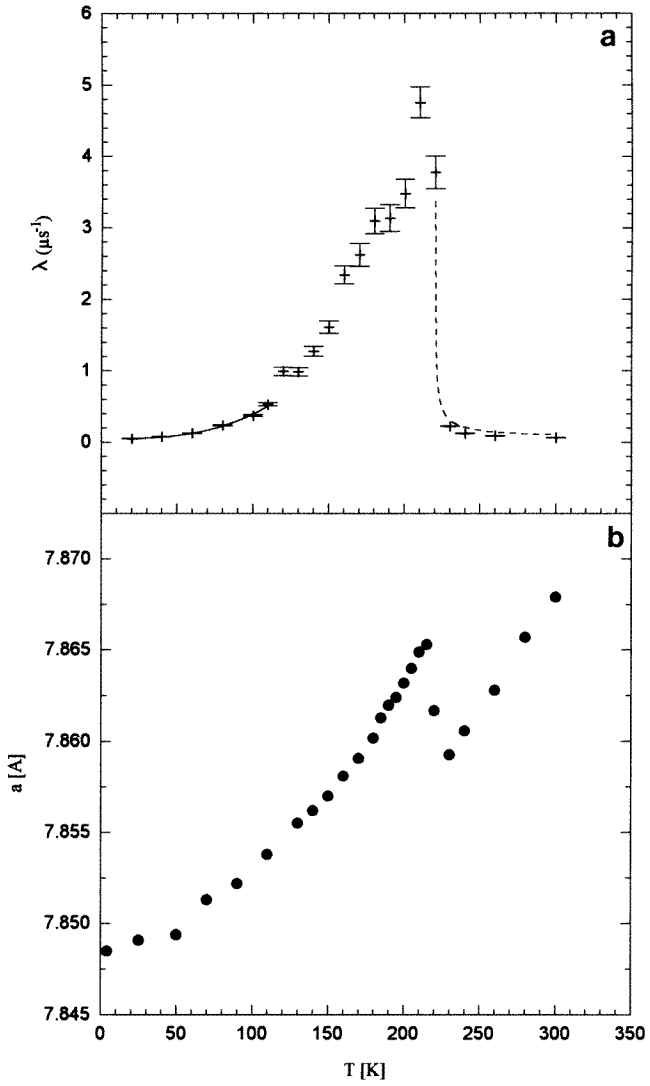

Figure 4. (*a*) The temperature dependence of the depolarization rate $\lambda(T)$ for YMn_2D_1. The solid line represents a fit to $\lambda(T) = \beta_0 T^3$ with $\beta_0 = 0.0214$ (± 0.0012). The broken line represents a fit to equation (7). The resulting parameters are listed in table 1. (*b*) The thermal expansion of YMn_2D_1 from [5].

proved sensitive to the magnitude of the external longitudinal field. A typical response for the YMn_2D_2 sample at 280 K is shown in figure 6. λ decreases rapidly as the field increases to 5 mT but remains approximately constant as the field increases further. In an applied field, λ retains its characteristic divergence towards T_c, as can be seen in figure 7 where $\lambda(T)$ is shown for YMn_2D_2 in a longitudinal field of 10 mT.

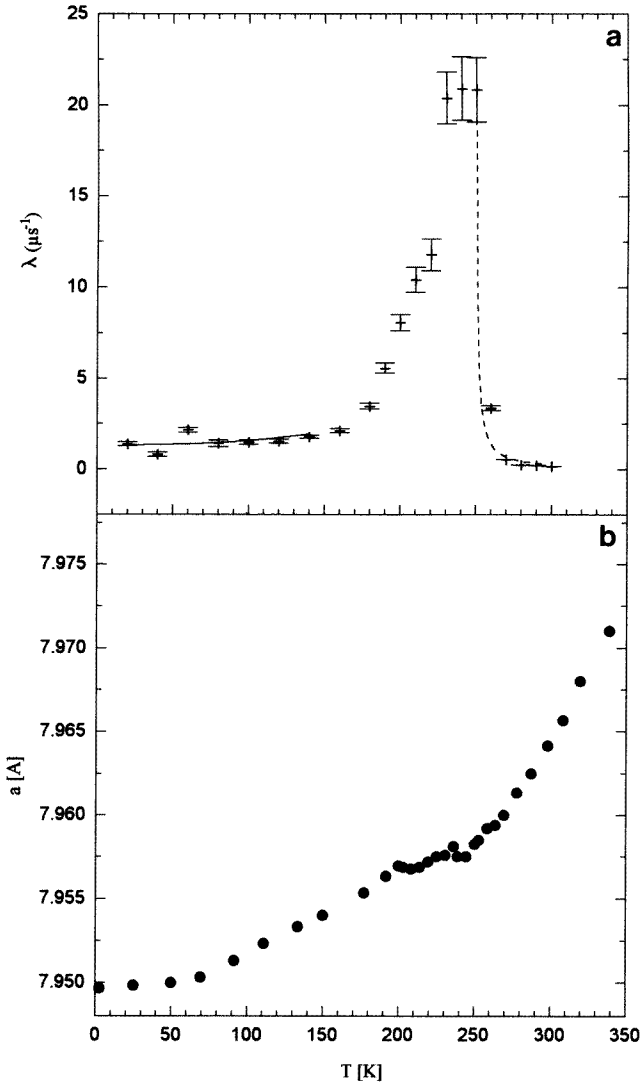

Figure 5. (*a*) The temperature dependence of the depolarization rate $\lambda(T)$ for YMn_2D_2. The solid line represents a fit to $\lambda(T) = \beta_0 T^3$ with $\beta_0 = 0.0096$ (± 0.011). The broken line represents a fit to equation (7). The resulting parameters are listed in table 1. (*b*) The thermal expansion of YMn_2D_2 from [6].

4. Discussion

The transition to the magnetically ordered state of the parent compound YMn_2 is of first order [3, 7]. The temperature variation is the μSR asymmetry term a_1 and the magnetization of the YMn_2 deuterides indicate that the transition to the magnetically ordered state remains discontinuous upon incorporation of deuterium into the lattice. This is illustrated graphically in figure 8, where the temperature dependence of the asymmetry a_1 is modelled assuming contributions from two coexisting phases, one magnetically ordered and the other

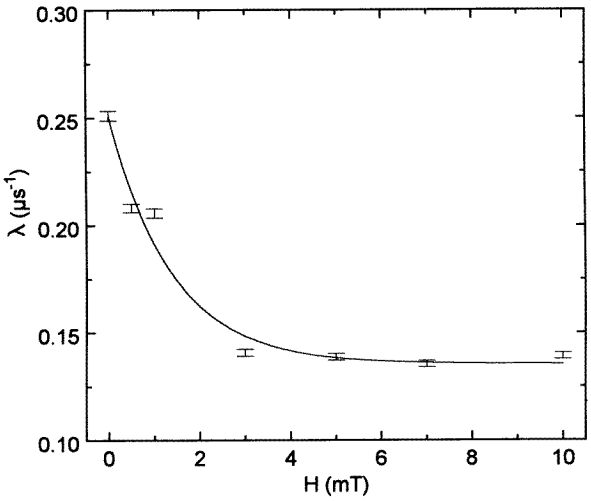

Figure 6. The variation in λ ($T = 280$ K) with applied longitudinal field for YMn_2D_2.

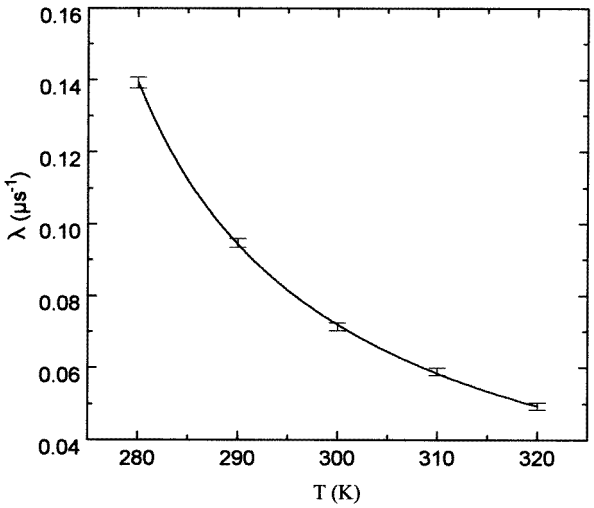

Figure 7. The temperature dependence of $\lambda(T)$ for YMn_2D_2 measured in an applied longitudinal field of 10 mT.

paramagnetic. The magnetically ordered state dominates at low temperatures and provides a term associated with the longitudinal dynamic depolarization term $G_-(t)$ of equation (3), i.e.

$$a_m = a_{1p}\{M(T')/M(0)\}/3 \tag{4}$$

where $M(T')/M(0)$ is the normalized magnetization which represents the volume fraction of the magnetically ordered part of the sample. a_{1p} is the asymmetry parameter in the paramagnetic state well above T_c. At high temperatures the paramagnetic state dominates

and contributes

$$a_p = a_{1p}[1 - \{M(T')/M(0)\}] \tag{5}$$

to the total asymmetry. Thus, at any temperature T,

$$a_1(T) = a_m + a_p = a_{1p}[1 - 2\{M(T')/M(0)\}/3]. \tag{6}$$

Note that, in the above expressions, $T' = T + \Delta T$ is an adjusted temperature, where ΔT for the slight shift in T_c between the value measured by μSR and that determined by magnetization measurements. A ΔT of approximately 10 K is extracted from a least-squares fit of equation (6) to the asymmetry data; this discrepancy may arise from hysteresis associated with the discontinuous character of the transition. It can be seen in figure 8 that the two-state model adequately describes $a_1(T)$ for both the YMn_2D_1 and the YMn_2D_2 samples.

The variation in λ with temperature provides direct information on the spin dynamics in YMn_2D_1 and YMn_2D_2. $\lambda(T)$ can be analysed within the theoretical framework established by Lovesey *et al* [14, 15], by considering three temperature regimes.

(i) $T < T_c/2$: In this low-temperature regime, the principal processes arise from the fluctuation of dipolar or hyperfine fields, and the excitation of spin waves. For dipolar field fluctuations and spin waves, λ is expected to vary as T^3, whereas a $T^{5/2}$ dependence is predicted for hyperfine field fluctuations. Within experimental uncertainties we cannot distinguish between these two possibilities. However, assuming that $\lambda(T) = \beta_0 T^3$, we find that $\beta_0 = 0.0214$ and 0.0096 μs^{-1} K^{-3} for YMn_2D_1 and YMn_2D_2, respectively. The larger β_0 observed for the YMn_2D sample is consistent with the smaller ferromagnetic component and the lower ordering temperature of this compound, both of which are expected to result in a enhanced field and spin fluctuations.

(ii) $T_c/2 < T < T_c$: Within this temperature range it is expected that $\lambda(T)$ varies as T^2, independent of the details of the source of relaxation. The experimental points approximately follow this functional form. However, we note that for both YMn_2D_1 and the YMn_2D_2 there is a characteristic anomaly below T_c. This anomaly may be related to the details of the thermal expansion curves, shown in figures 4(*b*) and 5(*b*). Details of the low-temperature magnetic structures of the YMn_2D_1 and YMn_2D_2 compounds, and their variation with temperature, have yet to be established. It is therefore not possible at present to distinguish whether the observed anomalies in $\lambda(T)$ are related simply to a structural transition or to the presence of a correlated structural and magnetic transition.

(iii) $T > T_c$: Despite the discontinuous nature of the magnetic transition at T_c, an extended critical divergence of $\lambda(T)$ characteristic of a continuous transition is observed in the paramagnetic regime. As in the case of the parent compound YMn_2 [8], the temperature dependence of λ may be expressed in terms of the critical form

$$\lambda(T) = \lambda_0[(T - T_c)/T_c]^{-\gamma} \tag{7}$$

from which the parameters shown in table 1 have been extracted for the YMn_2D_1 and YMn_2D_2 compounds. A shift $\Delta T = 10$ K in the transition temperature from that determined by magnetization measurements but consistent with that observed from the transition in a_1 is noted. Also shown in table 1 are the parameters obtained from a similar critical scaling analysis of the μSR measurements on YMn_2 [8]. It is also worth noting that the coefficient γ does not change in the field of 10 mT for the sample with $D = 2$ [16].

According to the theoretical description by Lovesey *et al* [14, 15], in general the critical behaviour of the muon depolarization in the paramagnetic phase arises predominantly from temporal fluctuations of the hyperfine fields. In YMn_2 itself the divergence of $\lambda(T)$ at T_N

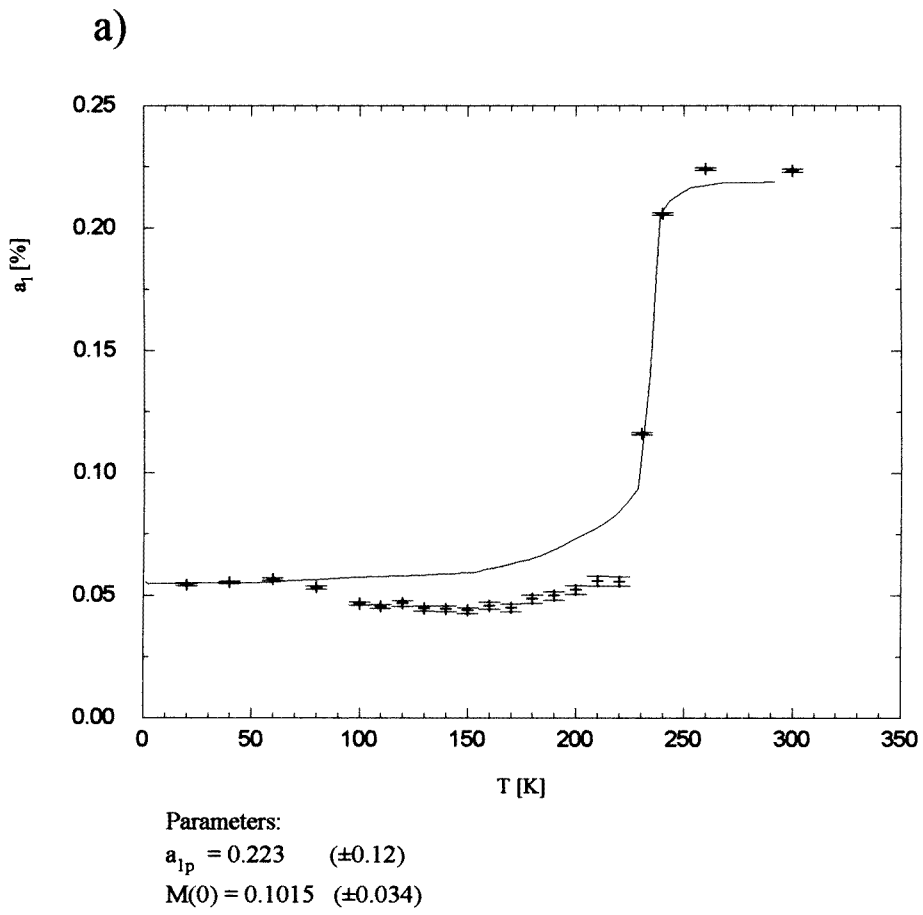

Figure 8. A fit of the two-magnetic-state model of equation (6) to the temperature variation of the total asymmetry a_1 for (*a*) YMn_2D and (*b*) YMn_2D_2. (*a*) The resulting parameters are $a_{1p} = 0.223$ (± 0.12) and $M(0) = 0.102$ (± 0.034). (*b*) The resulting parameters are $a_{1p} = 0.218$ (± 0.09) and $M(0) = 0.095$ (± 0.029).

has been discussed in terms of a critical slowing down of longitudinal (amplitude) spin fluctuations associated with the approach to localization of the itinerant Mn moments. The critical scaling of $\lambda(T)$ for the deuterides studied here suggest a characteristic depolarization rate λ_0 of 0.03 μs^{-1}, remarkably close to that of YMn_2 itself [8]. This value is relatively small and indicates that the associated spin fluctuations are rapid. It is particularly interesting that the magnitude of λ_0 is apparently independent of deuterium concentration, remaining constant for the YMn_2, YMn_2D_1 and YMn_2D_2 compounds, thereby implying that the character of the spin fluctations is unchanged by deuterium loading. However, thermal expansion measurements prove that hydrogen (deuterium) suppresses spin fluctuations. Moriya's [17] self-consistent renormalization theory of spin fluctuations in itinerant magnets relates the coefficient of thermal expansion to the amplitude of the longitudinal spin fluctuations; the thermal expansion coefficients are found to be closely similar for the YMn_2D_1 and YMn_2D_2 compounds, but smaller than for YMn_2 [5, 6]. This discrepancy presumably arises because λ_0 is estimated at the temperature range close to the ordering

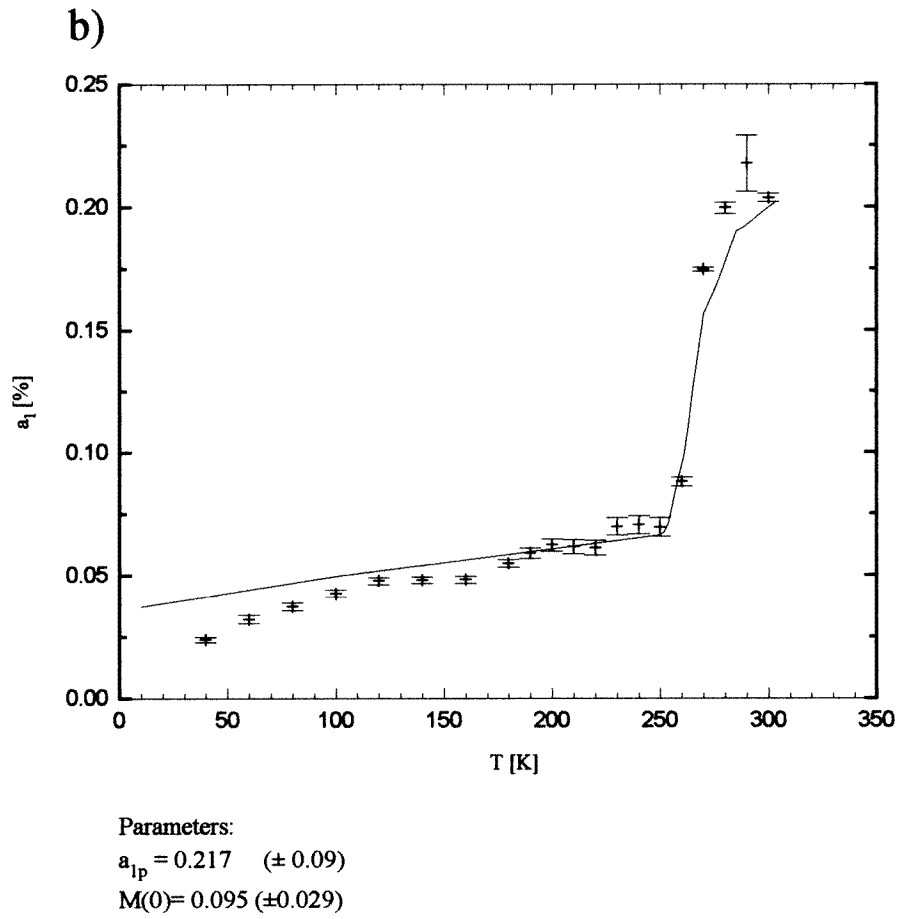

Figure 8. (Continued.)

temperature, whereas the thermal expansion coefficient is taken for temperatures well in the paramagnetic state.

Table 1. Parameters extracted from the critical scaling analysis of the muon depolarization rate $\lambda(T)$, according to equation (7) for YMn_2D_x compounds with $x = 1$ and $y = 2$. The parameters for $x = 0$ are taken from [8].

x in YMn_2D_x	λ_0 (μs^{-1})	T_c (K)	γ
0	0.033	92.5–113	0.35
1	0.0307(8)	219.2(4)	0.64(1)
2	0.0318(9)	258.6(1)	0.87(1)

In contrast with λ_0, the critical exponent γ changes markedly with deuterium concentration, rising from 0.3 for YMn_2 and reaching 0.87 for YMn_2D_2. Theoretically, the critical exponent itself cannot be related directly to details of the spin fluctuation spectra

or to the fluctution mechanisms.

The variation in γ with concentration is not understood. The critical scaling analysis of equation (7) should be considered in a more general context [15]. In reality, λ may be expressed as the sum over the Brillouin zone:

$$\sum_q \frac{\chi(q)}{\Gamma(q)} \tag{8}$$

where $\chi(q)$ is the wavevector-dependent susceptibility and $\Gamma(q)$ is a q-dependent width of the spin-fluctuation excitation spectrum. Both these quantities may be assumed to be extremely sensitive to deuterium concentration, which causes a related increase in interatomic distances and changes in magnetic interaction between Mn moments. Significant changes in the temperature dependence of $\chi(q)$ and $\Gamma(q)$ will hence be reflected in the temperature dependence of λ. A clarification of this problem must therefore await complementary inelastic neutron scattering measurements.

We also suggest that the marked suppression of the muon depolarization rate at modest fields (less than 5 mT) observed in these measurements on paramagnetic YMn_2D_1 and YMn_2D_2 is not attributable to the decoupling of the muon spin from nuclear moments, as is generally assumed, but instead is related to the effective longitudinal alignment of magnetic clusters above T_c.

5. Conclusions

In conclusion, our μSR measurements have enabled us to characterize the spin dynamics of YMn_2D_1 and YMn_2D_2 in both the paramagnetic and the magnetically ordered states. It appears that the longitudinal spin fluctuations which dominate the paramagnetic state of the parent compound YMn_2 persist, essentially unchanged in character, to relatively high deuterium concentrations. A critical divergence of the muon depolarization rate $\lambda(T)$ associated with the spin fluctuations is observed, while the temperature variation in the asymmetry parameter a_1 indicates a discontinuous transition to long-range magnetic order. Again, both these features are similar to those observed in μSR studies of the parent component, thereby emphasizing the intrinsic similarities in the nature of the magnetic transition of YMn_2 and its deuterides, despite the marked changes to the magnetically ordered state resulting from deuterium incorporation.

Relatively little detailed information can be extracted from the μSR measurements on YMn_2D_1 and YMn_2D_2 below T_c, largely because of resolution limitations of the pulsed muon technique employed in this study. However, our measurements do provide an indication that considerable dynamic depolarization processes are present to temperatures well below T_c. The temperature dependence of the depolarization rate $\lambda(T)$ associated with these processes is in broad agreement with theoretical predictions. However, anomalies are also observed in $\lambda(T)$ at temperatures close to anomalies in the thermal expansion. The origin and nature of these anomalies await characterization by neutron diffraction.

Acknowledgments

R Cywinski acknowledges financial support from the Engineering and Physical Sciences Research Council. G Wiesinger acknowledges the support of the Austrian Science Foundation (grant S5604). The authors would also like to thank the staff of the ISIS muon group for their help and support in the course of the μSR measurements and M Escorne for magnetic measurements.

References

[1] Wiesinger G and Hilscher G 1991 *Magnetism of Hydrides, Handbook of Magnetic Materials* vol 6, ed K H J Buschow (Amsterdam: Elsevier)

[2] Latroche M, Paul-Boncour V, Przewoznik J, Percheron-Guégan A and Bourée-Vigneron F 1994 *Proc. Int. Symp. on Metal–Hydrogen Systems (Fuhi-Yoshida, Yamanashi, 1994)*; 1995 *J. Alloys Compounds* **231** 99–103

[3] Shiga M, Wada H and Nakamura Y 1983 *J. Magn. Magn. Mater.* **31–4** 119

[4] Lacroix C and Pinettes C 1995 *Physica* B **206–7** 11

[5] Figiel H, Zukrowski J, Gratz E, Rotter M, Lindbaum A and Makroysan A S 1992 *Solid State Commun.* **83** 277

[6] Figiel H, Lindbaum A, Kapusta Cz and Gratz E 1995 *J. Alloys Compounds* **217** 157

[7] Fuji H, Saga M and Okamoto T 1987 *J. Less-Common Met.* **130** 25

[8] Cywinski R, Kilcoyne S H and Scott C A 1991 *J. Phys.: Condens. Matter* **3** 6473

[9] Rainford B D, Cywinski R and Dakin S 1995 *J. Magn. Magn. Mater.* **140–4** 805

[10] Eaton G H, Clarke-Gayther M A, Scott C A, Cox S F J, Kilcoyne S H, Cottrell S P, Brown S R and Williams W G 1994 *Rutherford Appleton Lab. Report* RAL-94-077

[11] Kilcoyne S H, Brown S R, Cottrell S P, Johnston S D and Scott C A 1994 *Rutherford Appleton Lab. Report* RAL-94-109

[12] Schenck A 1985 *Muon Spin Rotation Spectroscopy* (Bristol: Hilger)

[13] Paul-Boncour V and Escorne M 1995 unpublished results

[14] Lovesey S W, Karsson E B and Trohidu K N 1992 *J. Phys.: Condens. Matter* **4** 2043

[15] Lovesey S W, Trohidu K N and Karsson E B 1992 *J. Phys.: Condens. Matter* **4** 2061

[16] Percheron-Guégan A, Latroche M, Cywinski R, Figiel H, Kapusta C and Wiesinger G 1994–5 *Rutherford Appleton Lab. Report* RAL-95-A127

[17] Moriya T 1985 *Spin Fluctuations in Itinerant Electron Magnetism* (Berlin: Springer)